Supplementary information for

How to make an ice stream

Yu Zhang, Steven Franke, Till Sachau, Daniela Jansen, Haibin Yang, Dian Li, Yuanbang Hu, Ilka Weikusat, and Paul D. Bons

Corresponding authors: Yu Zhang, yu.zhang@mnf.uni-tuebingen.de; Paul D. Bons, paul.bons@uni-tuebingen.de

The PDF file includes:

Supplementary Text
Tables S1 to S2
Figs. S1 to S23
References

Other Supplementary Materials:

Videos S1 to S4

Supplementary Text

Results of free-slip models

Several studies suggested that the basal ice at NEGIS and its surroundings is not frozen to the bedrock, but sliding due to the presence of meltwater and/or subglacial till[12, 13, 63]. As a basal friction law is not implemented in our Underworld2-model, we tested the effect of a free-slipping ice-bedrock interface. Keeping all other settings the same as in no-slip Models 1 and 2, we observe the formation of a single ice stream that extends to the divide (Model 4, Fig. S18; Model 5, Fig. S19). No branching occurs and the ice stream develops a bottleneck shape. Without basal friction, lateral stresses can be transferred over long distances, allowing a single, wide ice stream to develop. This shows that the limited lateral stress transfer with basal friction or a frozen bedrock constrains the width and branching of the developing ice stream.

We compare free-slip models of variable anisotropy parameters (k) as well, since the anisotropy effect can be better observed when bedrock constraint is not playing a role. Compared with Model 4 (k = 10), Model 6 (k = 100) shows a faster ice-stream evolution process with stronger shear margins (Fig. S20–S22). However, in the isotropic Model 7, there is no ice-stream formation on the slippery bed (Fig. S23).

Scale and limitation of our model results

The drainage basin of the Northeast Greenland Ice Stream (NEGIS) is about 16% of the total area of the Greenland Ice Sheet[64]. NEGIS extends over 500 km from three main outlet glaciers: Nioghalvfjerdsfjorden Glacier (NG), Zachariae Isstrøm (ZI), and Storstrømmen Glacier (SG), and to its onset near the ice divide in the interior of northern Greenland (Fig. 1). To be approximately the same scale as the flow area of NEGIS, the horizontal model size was originally designed as 400 × 500 km with the outflow gate of a total 100 km, and the inflow flux represents ice from the model's outside area which can be regarded as an extension of our model width. If the inflow (v_x) is 8.8 m/yr with an ice thickness (h_{ice}) of 2500 m, the extra model width (x_{ex}) would be equal to 146.67 km where the losing ice is compensated by ice precipitation (v_{pr}) of 0.15 m/yr ($v_x\, h_{ice} = v_{pr}\, x_{ex}$). For the asymmetric inflow of 11.734 m/yr and 5.867 m/yr, the extra widths would be equal to 195.57 km and 97.78 km separately. The total width of our modelling area would then be approximately 700 km.

To maximize the model resolution and accuracy of the anisotropy code[28, 29], we scale down the horizontal model size but also the outflow gate size by a factor of ten. Meanwhile, we define a low outflow velocity 100 m/yr. Considering the ice thickness of 2500 m in our model, the ice mass loss through per km gate can be comparable to around 250-m-height ice with a higher velocity of 1000 m/yr at the NEGIS front[8, 64]. However, the real velocities at the NEGIS front are variable through space and time and can reach up to more than 1000 m/yr[6]. A higher ratio of velocity and ice thickness would cause a higher vertical stretching rate and a lower effective viscosity. This means our ice viscosities near the ice front or downstream are possibly higher than reality[29].

Shear heating would also cause ice softness in shear margins and the basal ice[34, 65, 66], which we do not include in our model. According to Eq. 4, ice viscosity is, for example, 3 times lower when ice temperature increases from –30 °C to –3 °C, while ice viscosity can be up to 10 times lower when the anisotropy parameter increases from k = 10 (standard anisotropy model) to k = 100 (exaggerated anisotropy model). In the NEGIS shear margins, temperature anomalies are suggested to be only around 2 °C to 6 °C[25, 65]. Thus our exaggerated anisotropy models (k = 100) can well indicate the evolution of an ice stream with possibly lower ice viscosities in shear

margins. As for basal melting, we show model cases of free-slip bottom boundary, but the modelled free slip cannot yet equal meltwater channelling with variable basal frictions underneath an ice stream[13, 67].

Combining the above-mentioned factors, we propose the real NEGIS may have a faster evolution process than our standard model (no slip; $k = 10$). However, the time scale of our modelling is still in a reasonable range (Figs. S7 and S8), which conforms to the previous study of fold observation in radargrams and strain analysis that shear margins in the upper NEGIS were fully developed ca. 2000 years ago[37]. In addition, compared with exaggerated anisotropy models ($k = 100$; Figs. S13 and S20) and free-slip models (Figs. S18–S20), the ice-stream formation processes do not show thousands of years of differences, which means influences from small viscosity changes and a general bedrock slip are limited on the time scale of ice stream formation.

We also need to point out a boundary effect when shear margins develop close to y-walls in no-slip models (Figs. S4, S8 and S14). C-axes of particles that enter the model to simulate influx have, on average, the same orientation as the particles at the local boundary. When the shearing has rotated the CPO at the boundary, the c-axes of newly introduced ice particles will mimic this CPO, which can make the outer shear margin easier to migrate but not localize individually. In free-slip models, shear margins experience less boundary effect since the ice stream develops in the centre of the model. The dominant shear margin can be observed on each side of the ice stream (Figs. S18–S20), with a clear c-axis orientation difference compared to surrounding areas (Figs. S22).

Our modelling mainly aims to investigate the effect of ice anisotropy, with the hypothesis that this is the main factor that governs the formation and evolution of ice streams in general. Modelling the evolution of a specific ice stream is complicated and may require more work in the future, considering variable ice mass loss and surface accumulation through time and space, shear heating and basal melting, as well as improving model size, resolution and boundary effects.

Table S1.

Basic model set-up parameters and their values. The flow law parameters A_0 and Q and the transition temperature (–11 °C) refer to the dislocation-creep regime in Table 3 of Kuiper[55] which is modified after Goldsby and Kohlstedt[54].

Parameter	Value	Unit
Model size (x, y, z)	40000, 50000, 3000	m
Model element numbers	128, 32, 16	
Particle numbers of each element	≥ 30	
Thickness air	500	m
Thickness ice (cold ice & warm ice)	2500 (1667+833)	m
gate width	10000	m
Velocity outflow (v_y)	100	m/yr
Velocity symmetric inflow (v_x)	8.8	m/yr
Velocity asymmetric inflow (v_x)	11.734; 5.867	m/yr
surface accumulation rate (v_{pr})	0.15	m/yr
Temperature ice (T_{bed}; T_0)	-30 to -3	°C
Density ice (ρ)	917.51 to 921.41	$\mathrm{kg/m^3}$
Viscosity air	1.0×10^{10} (or 1.0×10^{9} depending on min ice viscosity)	$\mathrm{Pa \cdot s}$
A_0 ($T < -11$°C)	5.0×10^{5}	$\mathrm{MPa^{-4.0} s^{-1}}$
A_0 ($T > -11$°C)	6.96×10^{23}	$\mathrm{MPa^{-4.0} s^{-1}}$
Q ($T < -11$°C)	64	kJ/mol
Q ($T > -11$°C)	155	kJ/mol
R	0.008314	$\mathrm{J \cdot mol^{-1} K^{-1}}$
Stress exponent n	4.0	
Anisotropy parameter k	10; 100	

Table S2.
Summary and comparison of all models.

No.	Bed condition	Anisotropy parameter (k)	Inflow	Result for each model	Figure & Video lists
Model 1	No-slip	10	Symmetric	Tributary ice stream	Figs. S3–S6; Video S1
Model 2	No-slip	10	Asymmetric	Ice stream dominant in one direction (NEGIS-type)	Figs. S7–S12; Figs. 3–4; Video S2
Model 3	No-slip	100	Asymmetric	Ice stream dominant in one direction (NEGIS-type); faster and stronger compared to Model 2	Figs. S13–S17; Video S3
Model 4	Free-slip	10	Symmetric	Single ice stream perpendicular to the outlet	Fig. S18
Model 5	Free-slip	10	Asymmetric	Single ice stream perpendicular to the outlet	Fig. S19
Model 6	Free-slip	100	Symmetric	Single ice stream perpendicular to the outlet; faster and stronger compared to Model 4	Figs. S20–S22; Video S4
Model 7	Free-slip	Isotropy	Symmetric	No ice stream formation	Fig. S23

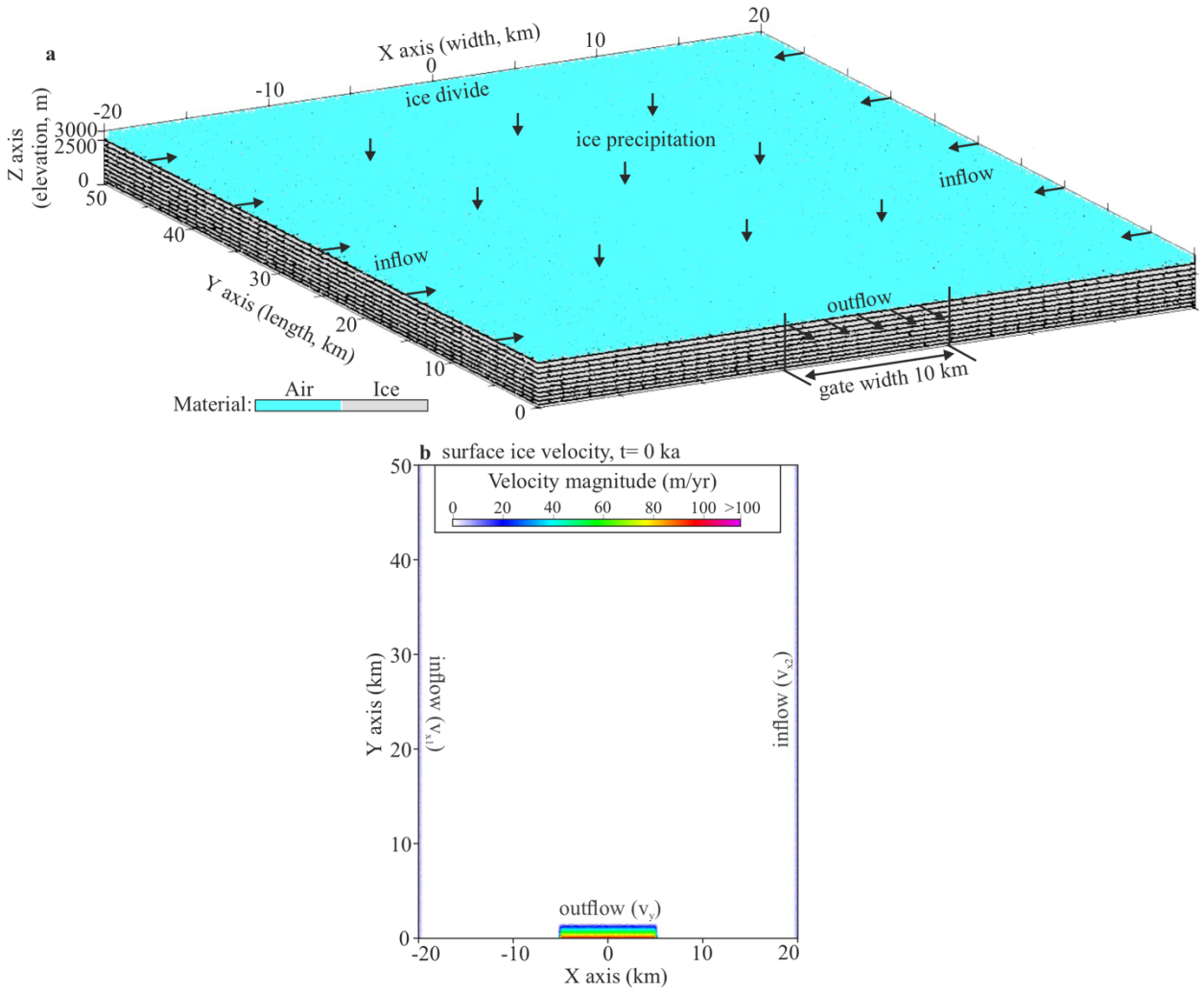

Fig. S1.

Model design. **a,** 3D view of an initial model at $t = 0$ ka. An outflow in the y-direction through the outlet at x-wall ($y = 0$ km) with a gate width of 10 km ($-5 \leq x \leq 5$ km). Ice precipitation on the ice surface and lateral inflow from y-walls ($x = -20$ & 20 km) to compensate for the outflow. Ice divide is the 0-velocity x-wall ($y = 50$ km). **b,** Surface ice velocity map at $t = 0$ ka (example from Model 1 with symmetric inflow).

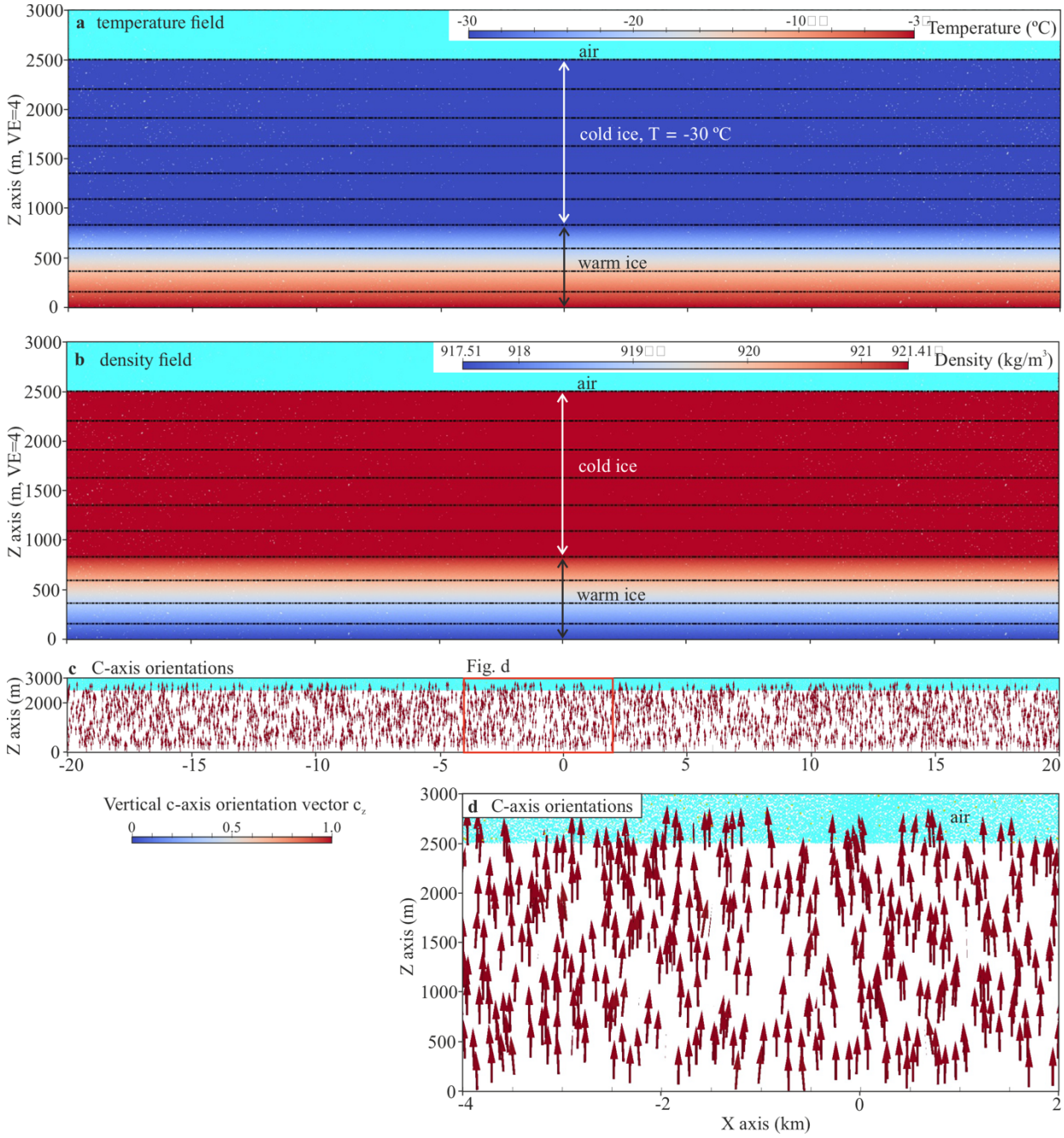

Fig. S2.

Initial physical settings. **a,** Vertical temperature field from –3 °C (T_{bed}) to –30 °C (T_0) at $z > 833$ m. **b,** Ice density field with a vertical gradient from 917.51 kg/m^3 (–3 °C) to 921.41 kg/m^3 (–30 °C). Note the vertical exaggeration (4×) in the temperature and density profiles. **c, d,** C-axis orientations (arrows) of ice particles. Arrow colours represent vertical vectors, with deep red being vertical (1.0).

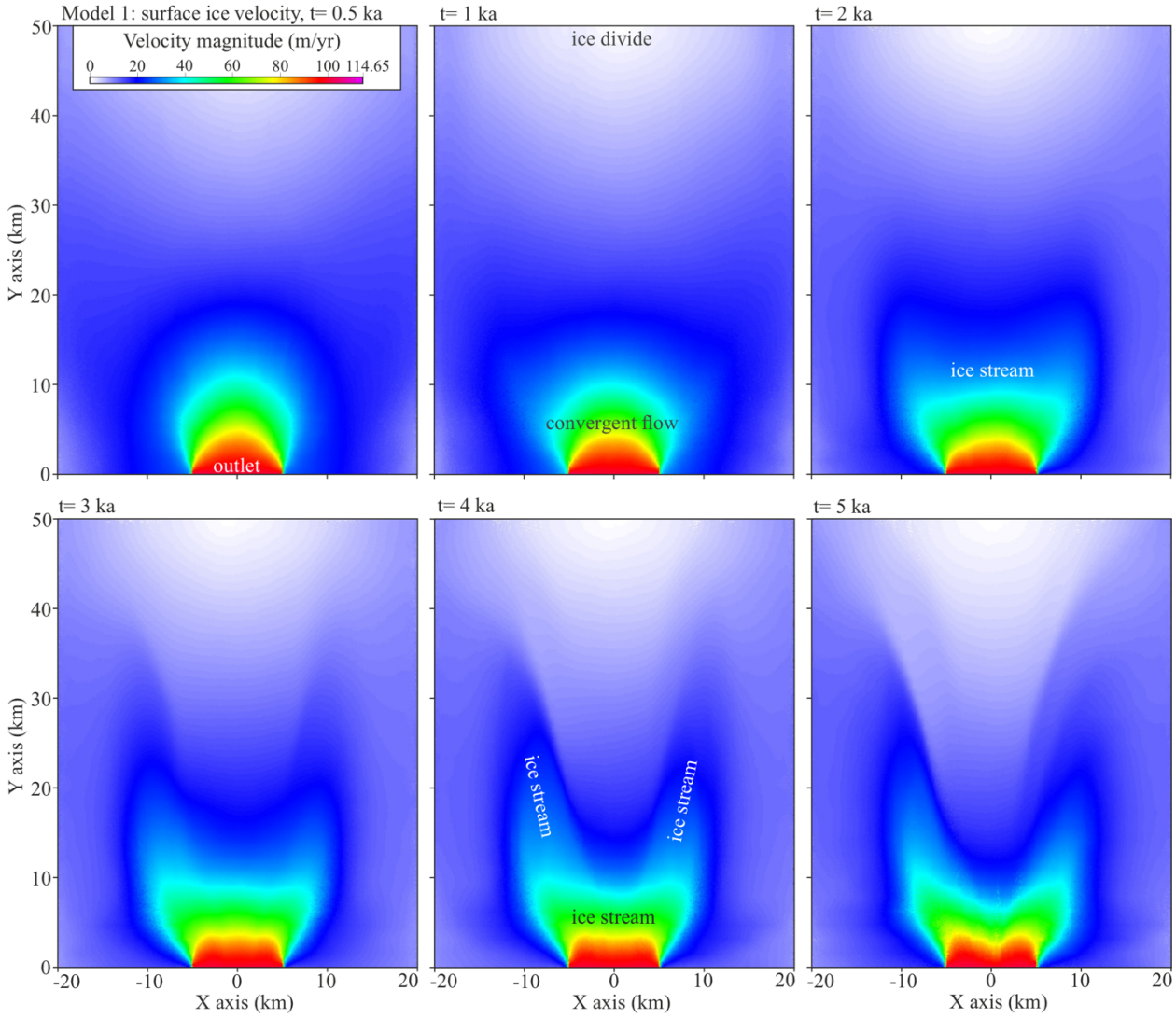

Fig. S3.

Evolution of surface ice velocities in Model 1 (no slip; symmetric inflow; anisotropy $k = 10$) from 500 to 5000 years. At the beginning, there is a convergent flow around the narrow outlet and ice velocities gradually decrease in surrounding ice. Between 1000 and 2000 years, the area of the fast ice flow narrows and develops a larger velocity difference with surrounding ice and forms the proto ice stream. From 2000 to 4000 years, the ice stream grows inland by two tributaries and gradually shows a clear velocity difference with surrounding ice. At 5000 years, the ice stream continues to change its shape and position slightly. Both tributaries become narrower and more oblique to the outlet.

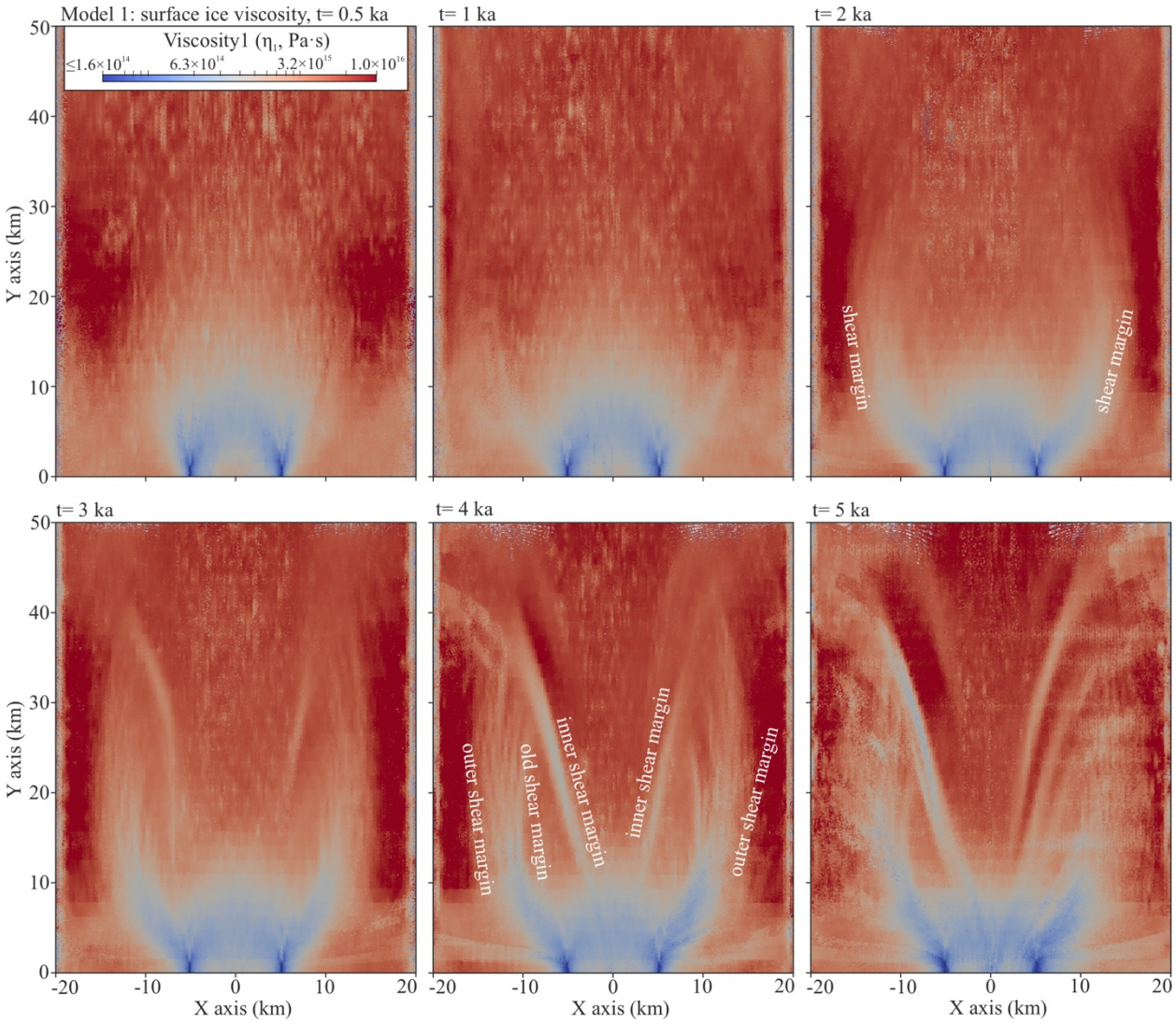

Fig. S4.

Evolution of general viscosities η_1 from the ice surface in Model 1 from 500 to 5000 years. Between 1000 and 2000 years, two shear zones (low viscosity area) develop in the convergent flow and become the shear margins of the proto ice stream. At 3000 years, the original shear margins grow inland, accompanied by inner shear margins established to form the tributaries of the ice stream. At 4000 years, shear margins of ice stream's tributaries are distinct. Shear margin migrations can be observed towards *y*-walls (x = –20 & 20 km). Shear margins of the two tributaries are near-symmetric but not identical due to the initial noises in c-axis orientations (Fig. S2c).

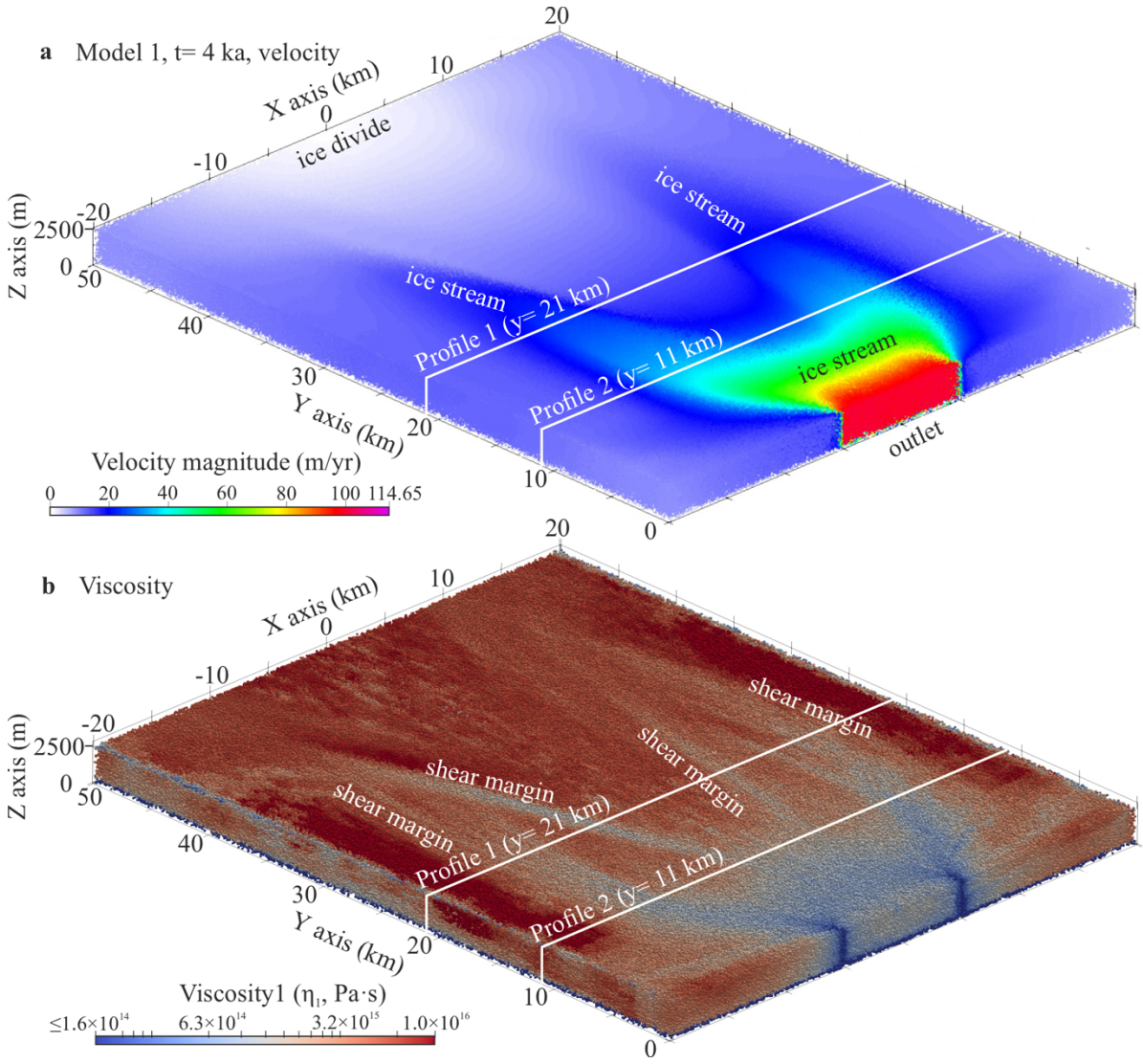

Fig. S5.

3D views of the tributary-type ice stream in Model 1 at 4000 years. **a,** Ice velocities. **b,** Ice general viscosities η_1.

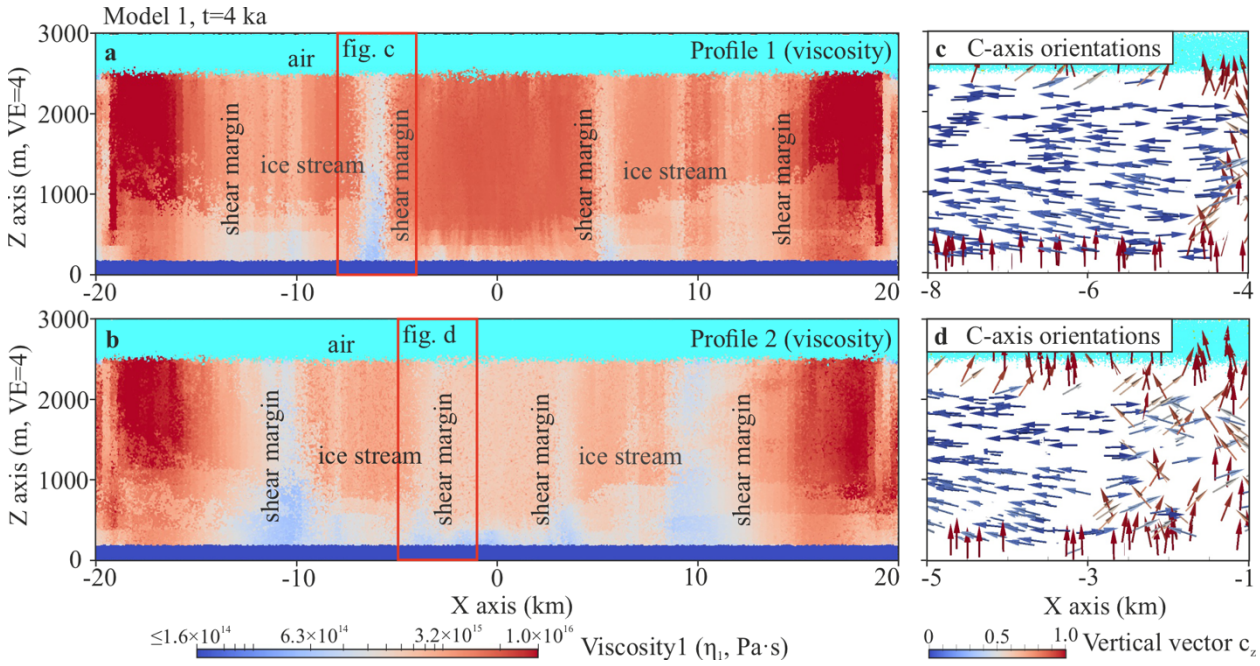

Fig. S6.

Profile snapshots of the tributary-type ice stream in Model 1 at 4000 years. **a, b,** Ice general viscosities η_1 on Profile 1 (**a**) and Profile 2 (**b**) transverse the ice stream (profile locations in Fig. S5). Note the vertical exaggeration (4×) in the profiles. **c, d,** C-axis orientations (arrows) of ice particles at the shear margin marked in profiles with red frames. Arrow colours represent vertical vectors. Viscosity profiles show two pairs of shear margins at the ice stream's tributaries. Vertical shear zones inside the tributaries are old shear margins. Taking an example from an inner shear margin, except for the basal ice, c-axis orientations of ice particles inside and around the shear margin are rotated into horizontal or small angles to the horizontal plane.

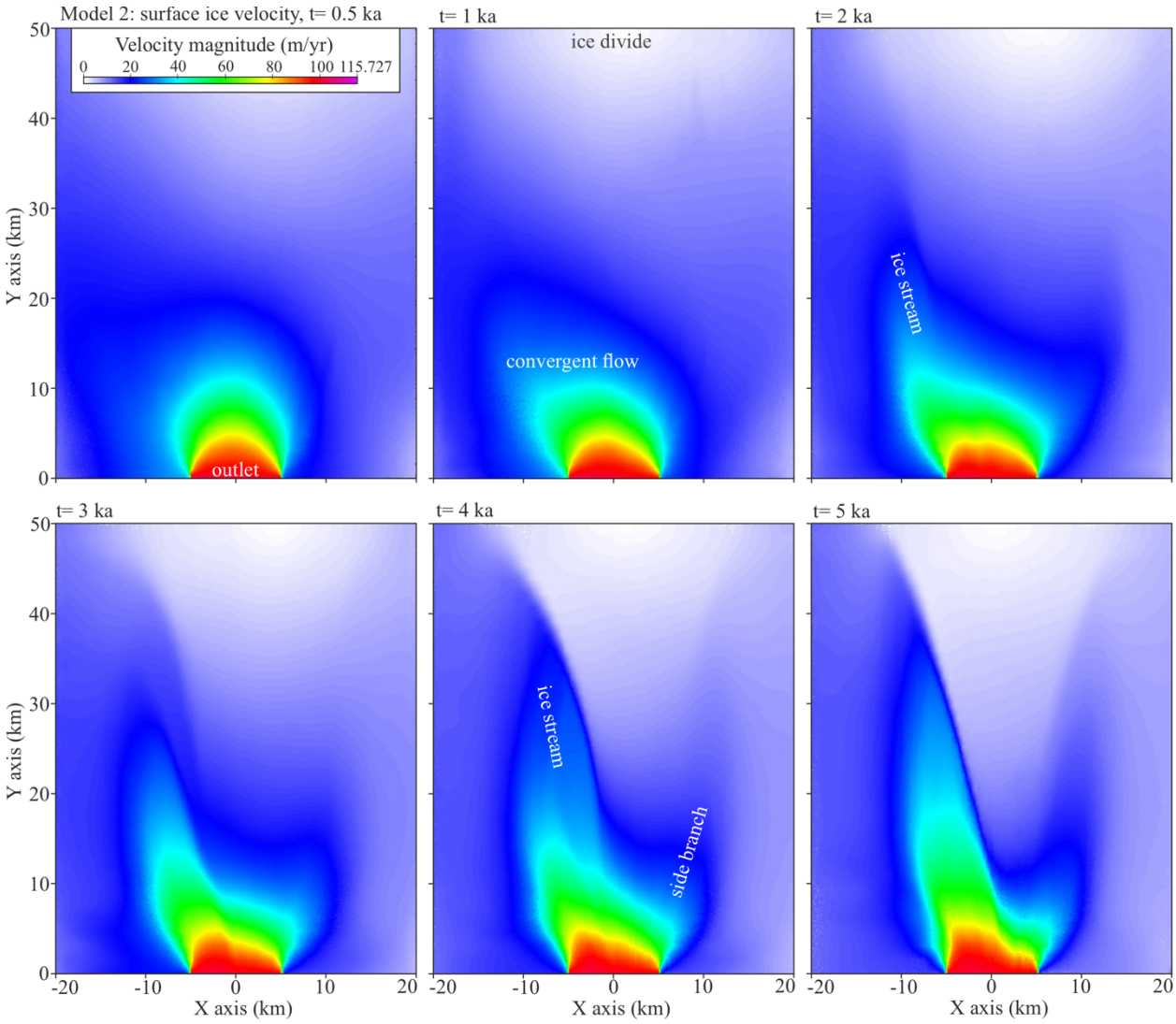

Fig. S7.

Evolution of surface ice velocities in Model 2 (no slip; asymmetric inflow; anisotropy $k = 10$) from 500 to 5000 years. The convergent flow around the narrow outlet is asymmetric at the beginning. Between 1000 and 2000 years, the fast ice flow develops along the higher ice inflow on the left side and forms the initial ice stream (NEGIS-type) with a weak branch on the other right side. At 4000 years, the ice stream grows farther inland and closes at the ice divide. From 4000 to 5000 years, the ice stream gradually narrows and develops a larger velocity difference with surrounding ice. The ice stream's position has a slight shift towards the model centre (left to right). The side branch is slowly developing as well.

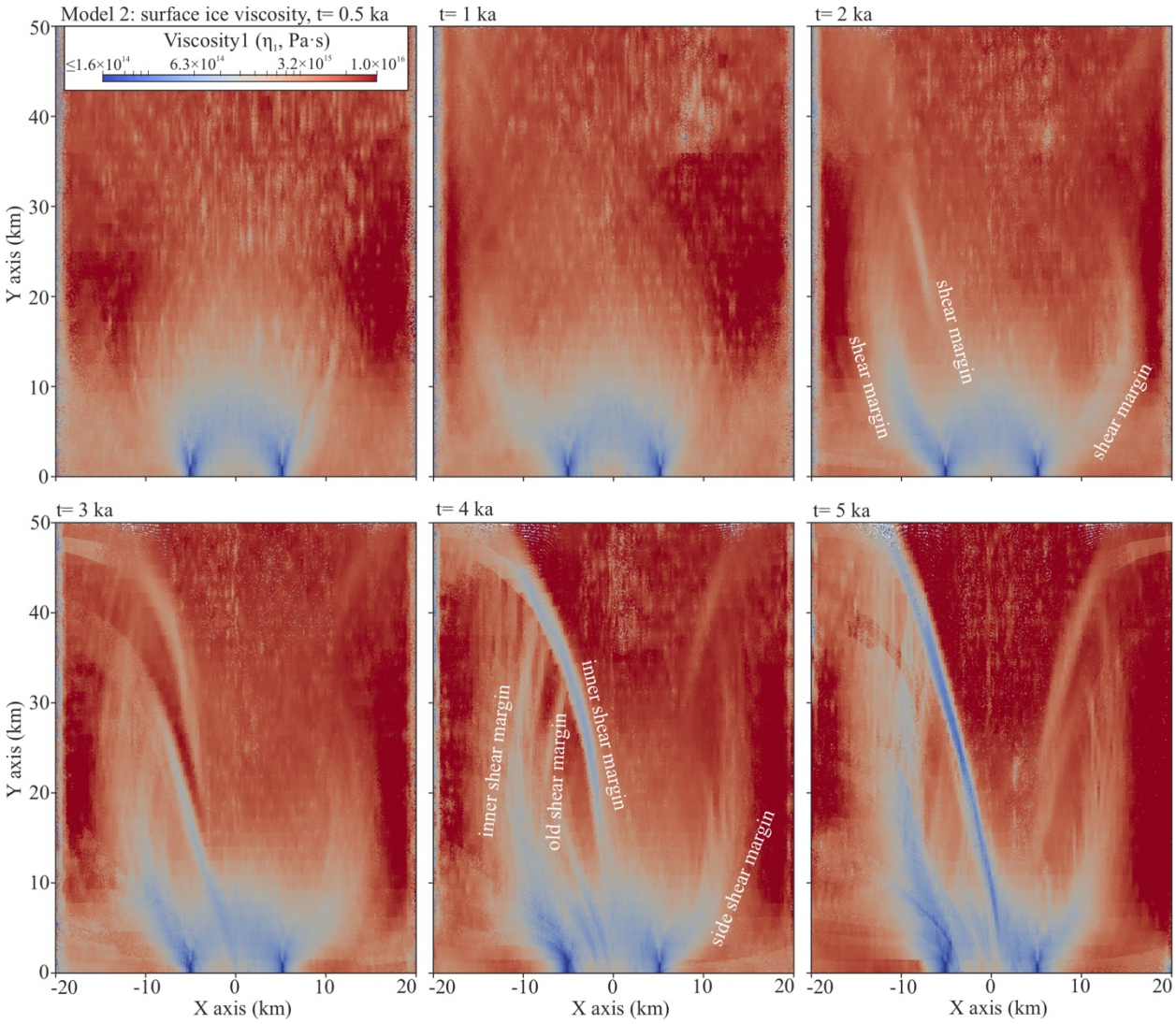

Fig. S8.

Evolution of general viscosities η_1 from the ice surface in Model 2 from 500 to 5000 years. At 1000 years, a shear zone develops firstly in the left part of the convergent flow. At 2000 years, the shear margins of the ice stream are established; the outer shear margin of the ice stream's side branch develops as well while the inner shear margin is not obvious. From 2000 to 4000 years, shear margins develop farther inland. Some old shear margins flow into the ice stream and new shear margins form around. Shear margin migrations are along with ice flow directions (Fig. S9), not the same as Model 1 (Fig. S4). At 5000 years, shear margins become more distinct, including at the ice stream's side branch. Some old shear margins inside the ice stream can be observed to have disappeared.

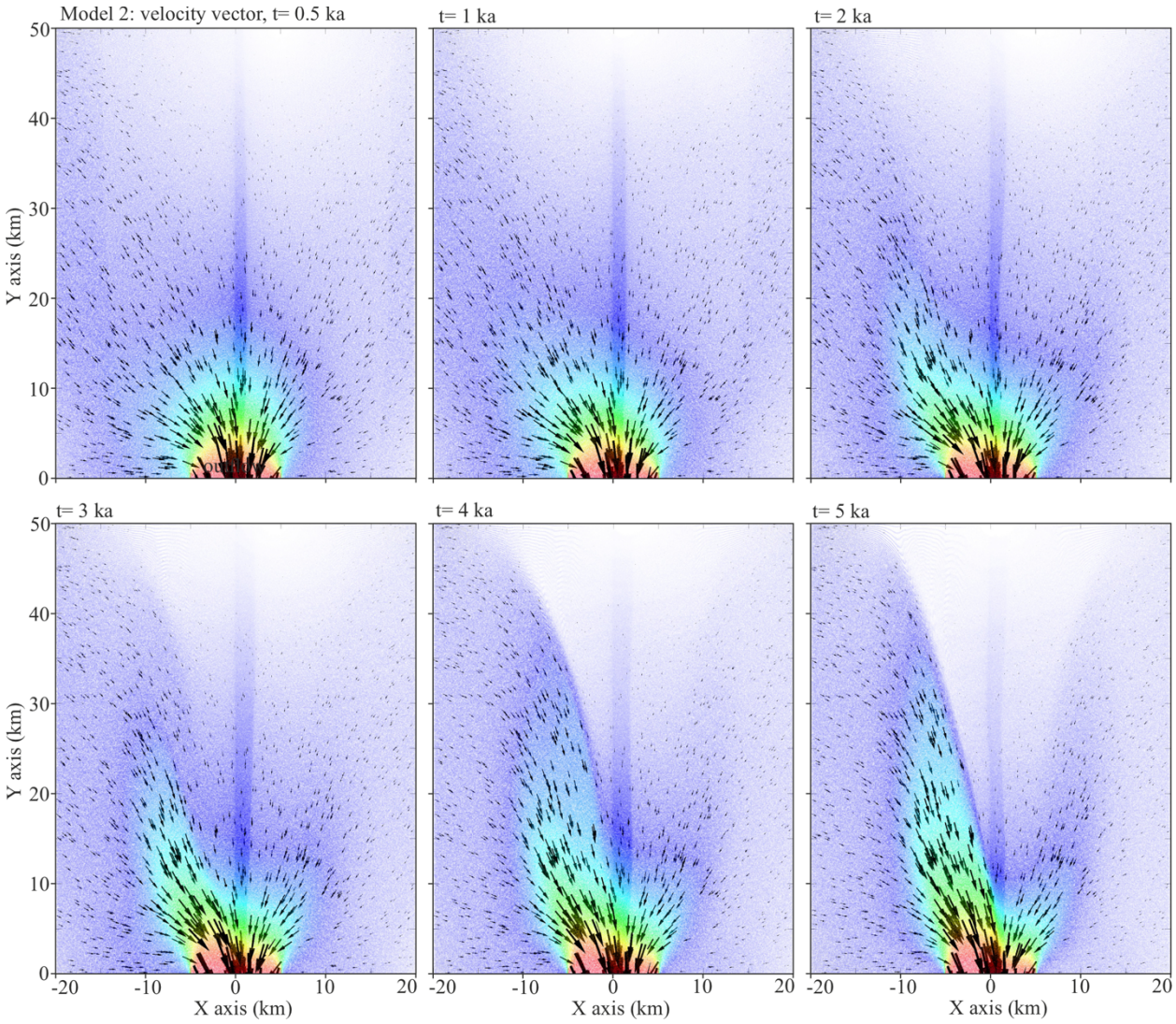

Fig. S9.

Top views of ice velocity vectors (arrows) in Model 2 from 500 to 5000 years. Arrow orientations point to ice flow directions. The arrow size is scaled with ice flow speed. Ice stream position is shown with the translucent velocity magnitude map from Fig. S7. Ice velocity vectors change through time along with the ice stream's evolution. The velocity vector field of the modelled NEGIS-type ice stream shows a similarity to the real NEGIS[13, 68].

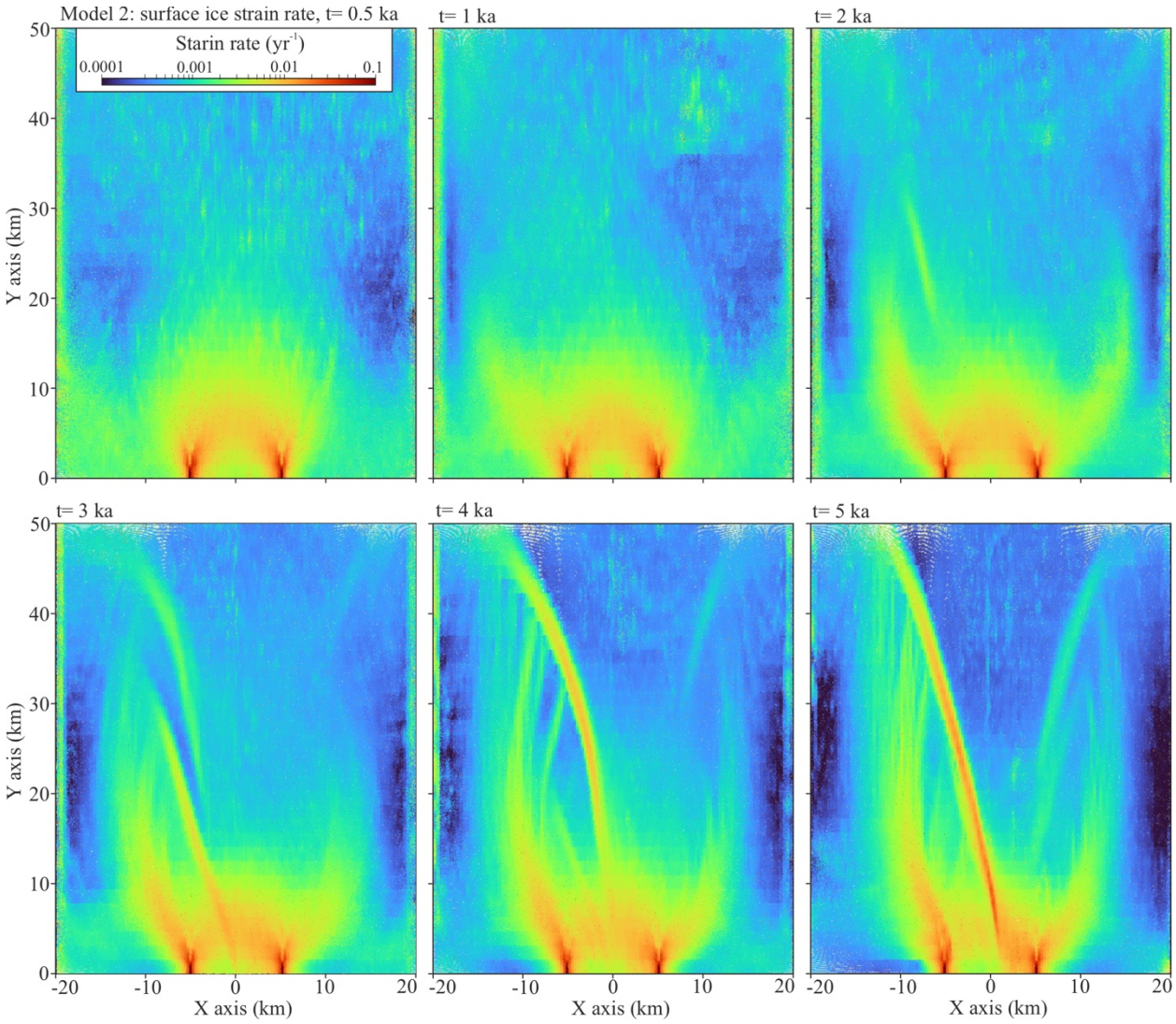

Fig. S10.

Top views of ice strain rates (the second invariant of strain-rate magnitude) in Model 2 from 500 to 5000 years. Shearing in shear margins can be observed in the high strain-rate areas with strain-rate values around 0.01 yr^{-1}. Except for a more dispersed pattern of the outer shear margin due to a boundary effect, the strain-rate map at 4000 years is comparable with the maximum shear strain rate map of real NEGIS[69].

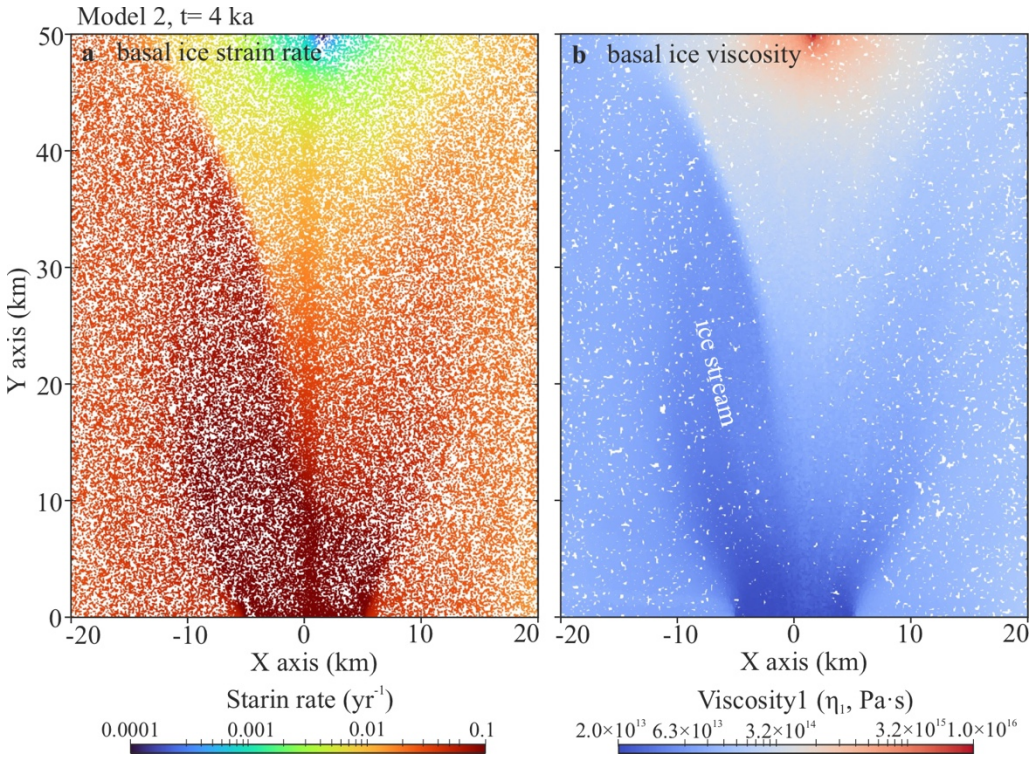

Fig. S11.

Properties of a basal ice layer (z = 100 m) at 4000 years in Model 2. **a,** Strain rates (the second invariant of strain-rate magnitude). **b,** General viscosities η_1. The basal ice on the no-slip boundary experiences bedrock-parallel shearing and strain softening along with the ice flow. It should be noted that the real basal environment would be more complicated considering shear heating, basal melting/freeze-on, and bedrock topography.

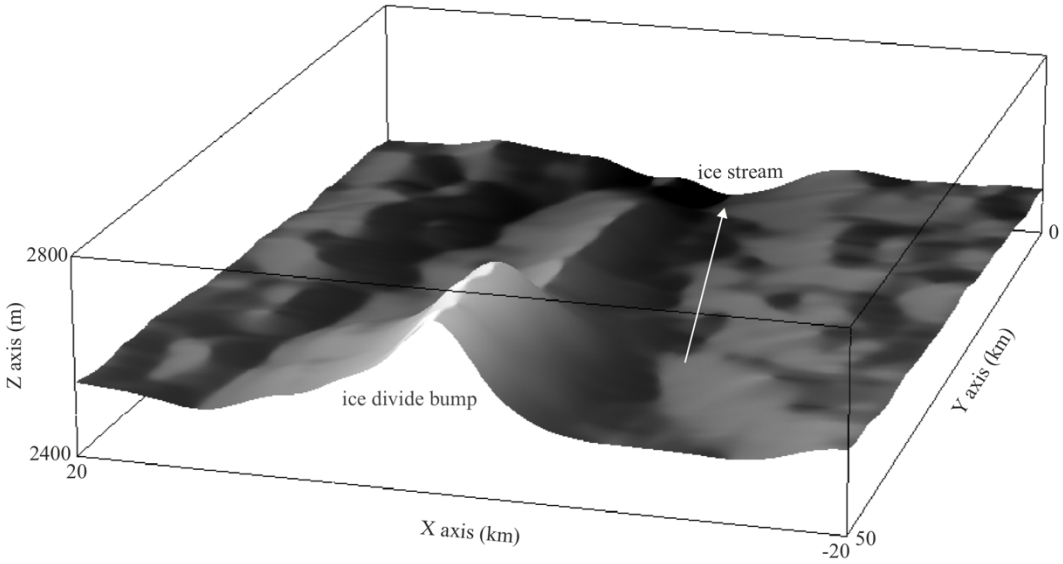

Fig. S12.

3D geometry of the ice surface in Model 2 at 4000 years. The bump at the ice divide has a similar mechanism to the Raymond bump[60, 70], which can also be indicated by the low strain rate and high viscosity area in Fig. S11. The shear-margin trough[71, 72] can be observed especially at the inner shear margin of the ice stream.

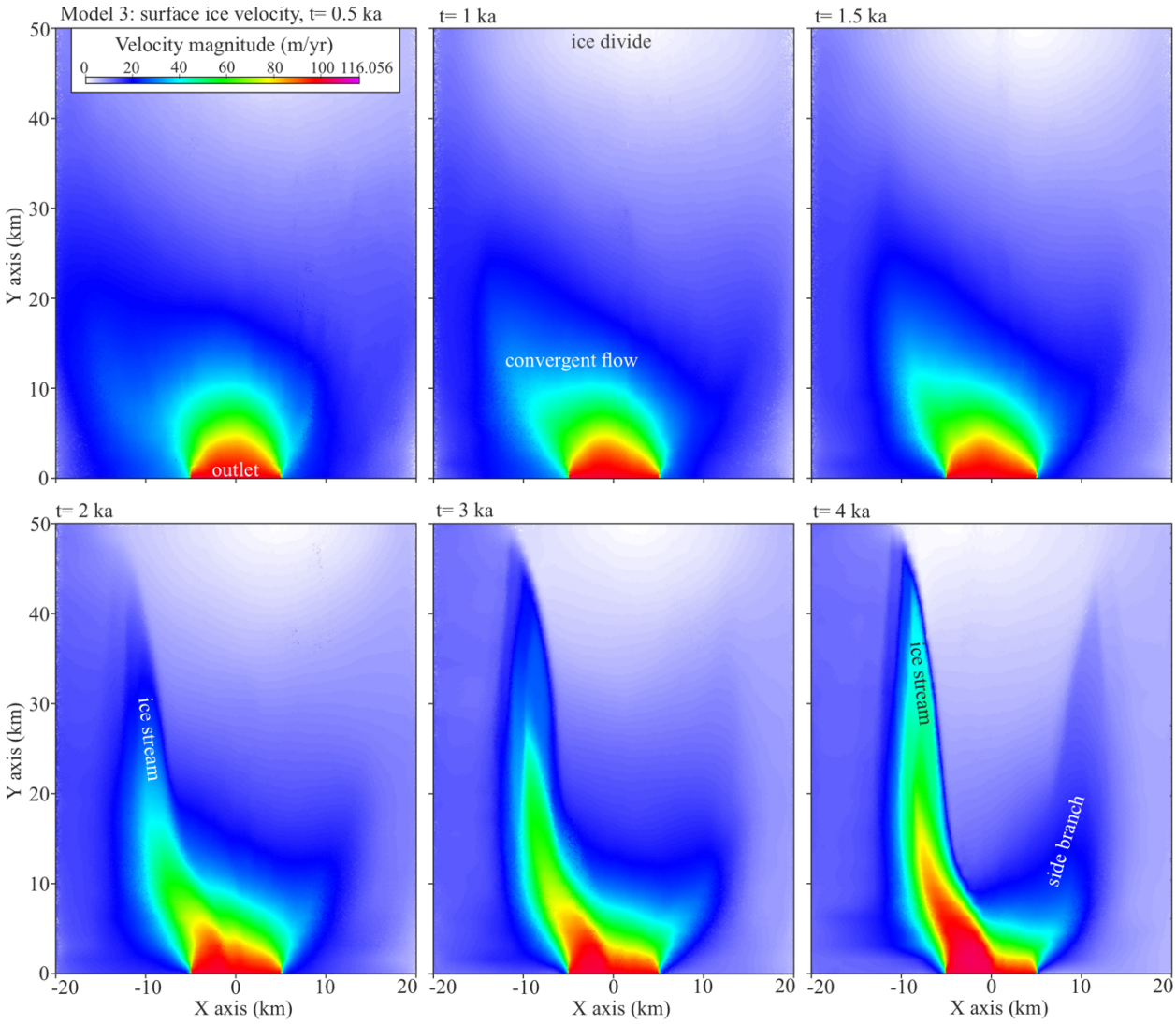

Fig. S13.

Evolution of surface ice velocities in Model 3 (no slip; asymmetric inflow; anisotropy k = 100) from 500 to 4000 years. The evolution process of the NEGIS-type ice stream in Model 3 is faster than in Model 2 (k = 10; Fig. S7). At 2000 years, the ice stream already exhibits a large velocity difference with surrounding ice. At 3000 years, the ice stream grows close to the ice divide. At 4000 years, the ice stream is narrower and has a much larger velocity difference with surrounding ice than in Model 2.

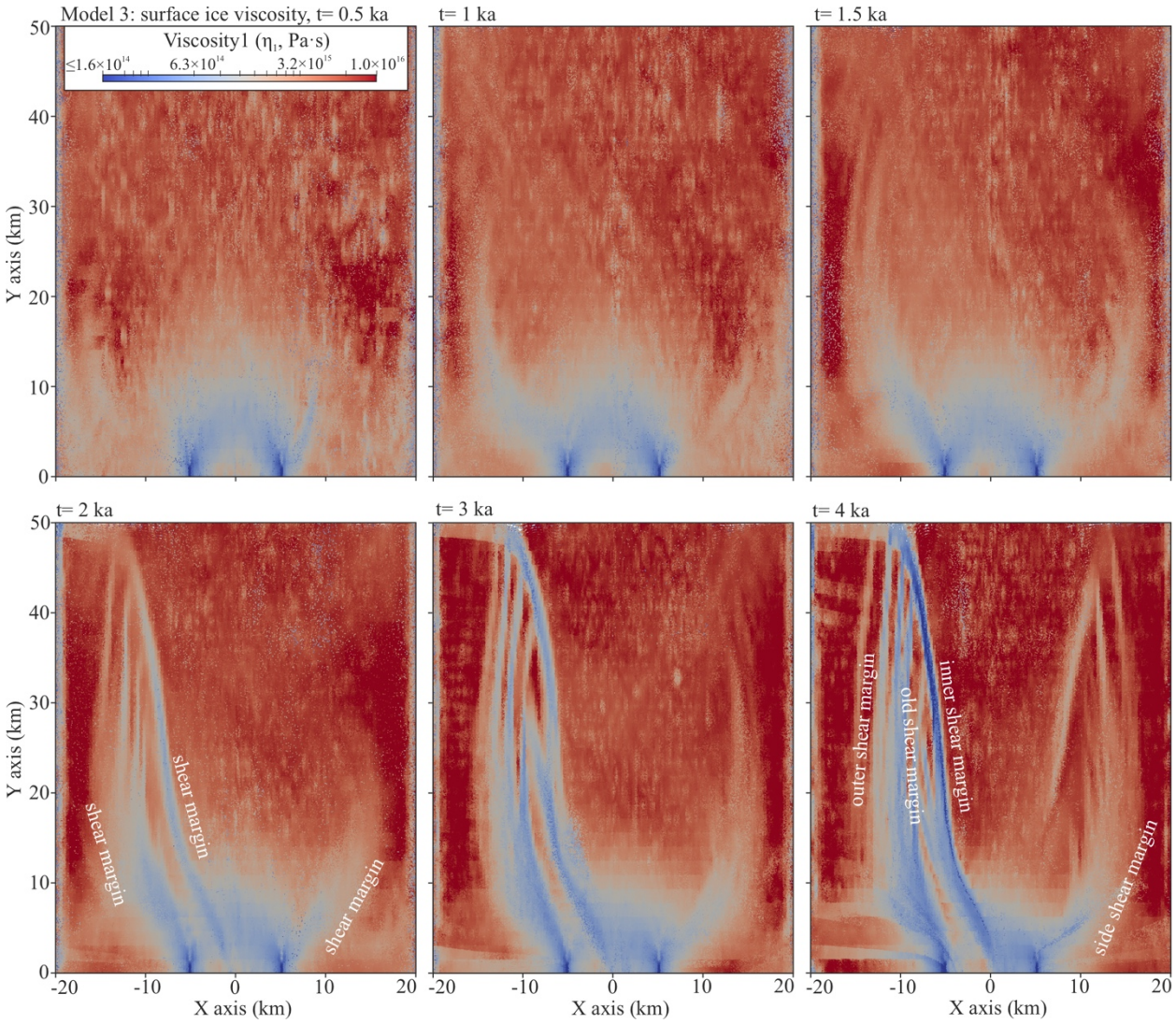

Fig. S14.

Evolution of general viscosities η_1 from the ice surface in Model 3 from 500 to 4000 years. At 2000 years, the shear margins of the ice stream are already established. At 4000 years, shear margins are softened more than in Model 2 (Fig. S8).

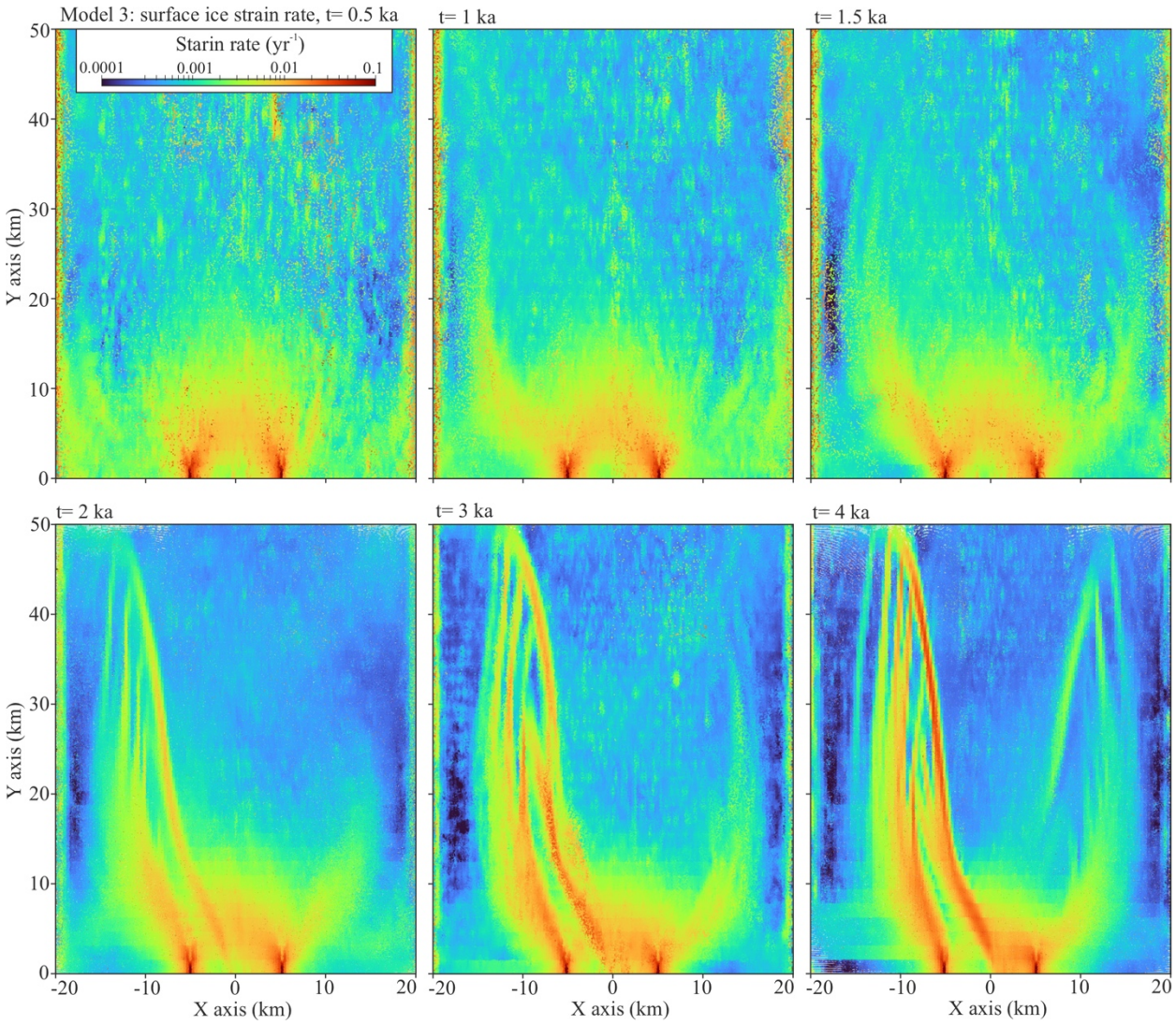

Fig. S15.

Top views of ice strain rates (the second invariant of strain-rate magnitude) in Model 3 from 500 to 4000 years. Strain rates in shear margins can be observed higher than in Model 2 (Fig. S10).

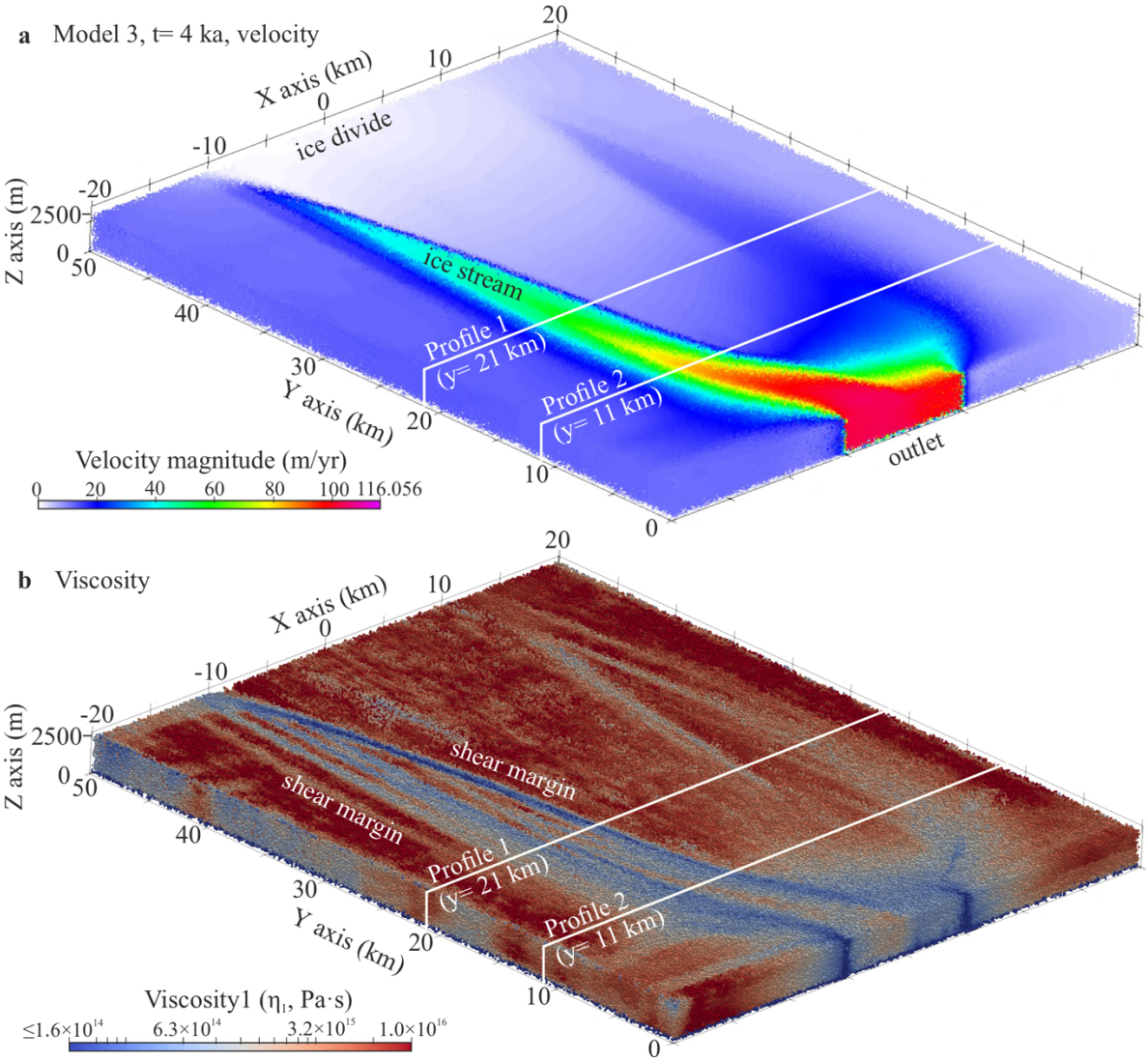

Fig. S16.

3D views of the NEGIS-type ice stream in Model 3 at 4000 years. **a,** Ice velocities. **b,** Ice general viscosities η_1.

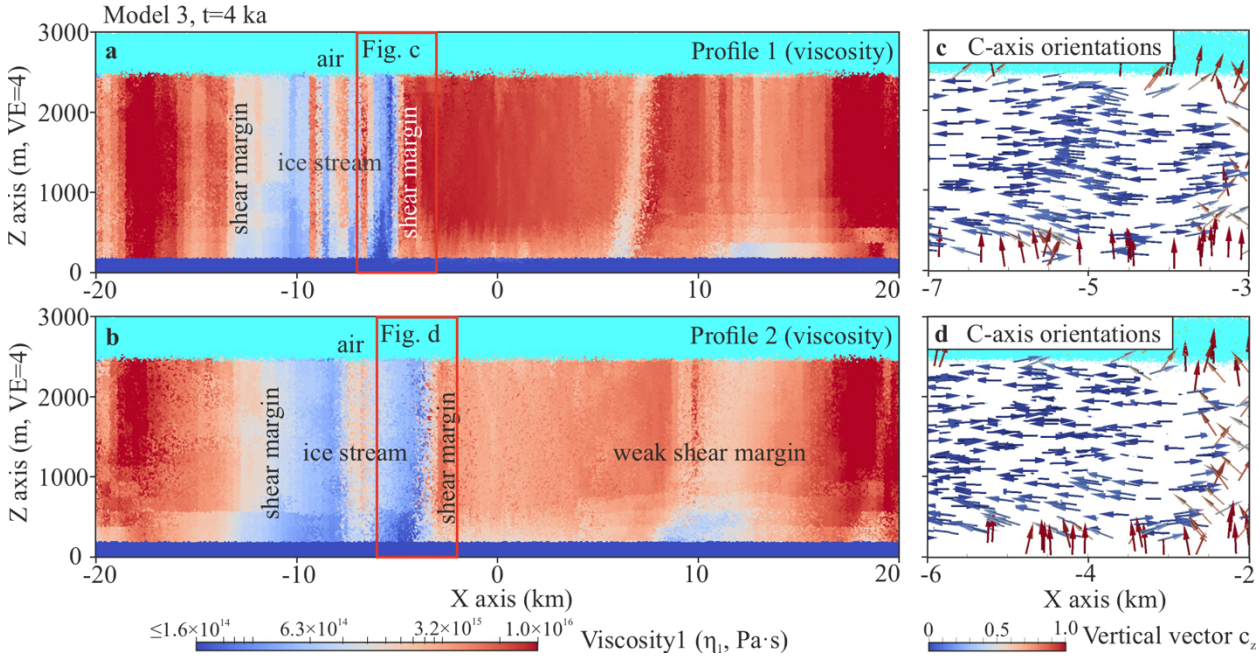

Fig. S17.

Profile snapshots of the NEGIS-type ice stream in Model 3 at 4000 years. **a, b,** Ice general viscosities η_1 on Profile 1 (**a**) and Profile 2 (**b**) transverse the ice stream (profile locations in Fig. S16). Note the vertical exaggeration (4×) in the profiles. **c, d,** C-axis orientations (arrows) of ice particles at the shear margin marked in profiles with red frames. Arrow colours represent vertical vectors. Shear margins (or old shear margins inside the ice stream) are indicated by vertical zones of strongly softened ice. Weak shear margin(s) can be observed at the ice stream's side branch as well. Except for the basal ice, the c-axis orientations of ice particles inside and around the strong shear margin are rotated into horizontal or small angles to the horizontal plane.

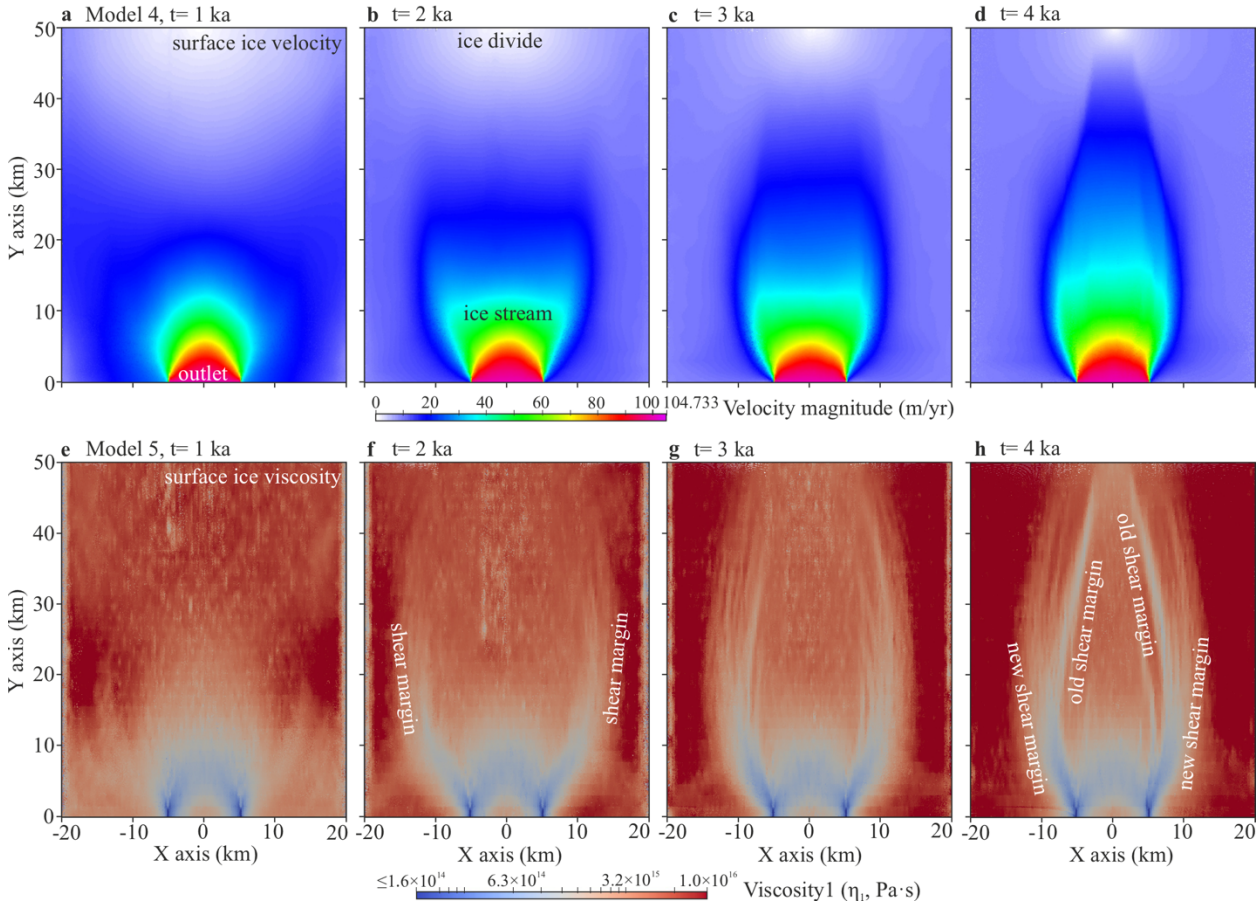

Fig. S18.

Evolution of surface ice velocities (**a–d**) and general viscosities η_1 (**e–h**) in Model 4 (free slip; symmetric inflow; anisotropy $k = 10$) from 1000 to 4000 years. The ice stream seems to quickly form between 1000 and 2000 years with its shear margins close to the ice divide. Compared with no-slip Model 1 (Figs. S3–S4), the ice stream does not later develop its tributaries but evolves along the outlet to the ice divide with a bottleneck shape. From 2000 to 4000 years, the single ice stream narrows its width; shear margins flow towards the centre of the ice stream accompanied by the gradual formation of new shear margins outside.

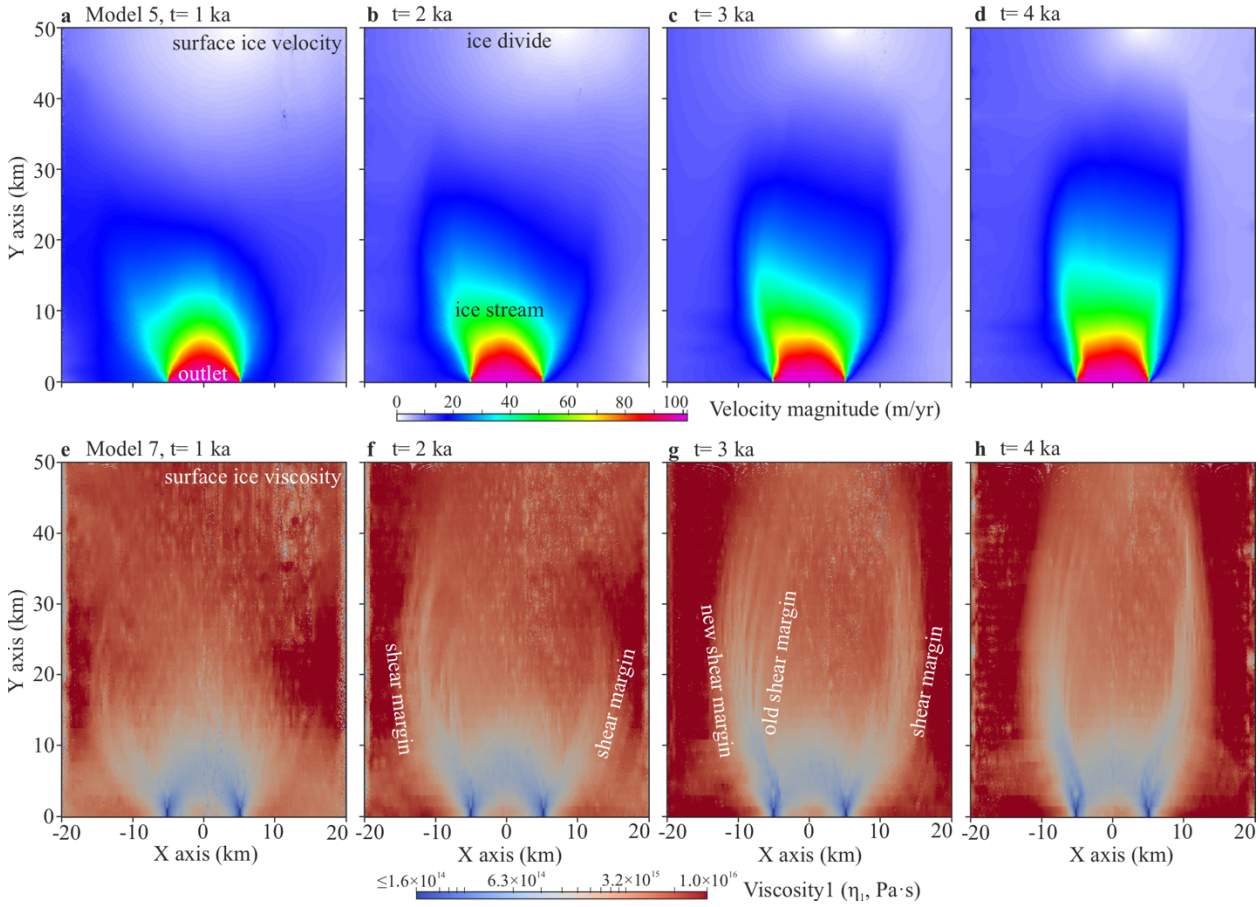

Fig. S19.

Evolution of surface ice velocities (**a–d**) and general viscosities η_1 (**e–h**) in Model 5 (free slip; asymmetric inflow; anisotropy k = 10) from 1000 to 4000 years. The ice stream is slightly asymmetric and the left shear margin (at the faster inflow side) migrates faster than the right one. Compared with no-slip Model 2 (Figs. S7–S8), the ice stream develops along the outlet and directly to the ice divide, without a side branch.

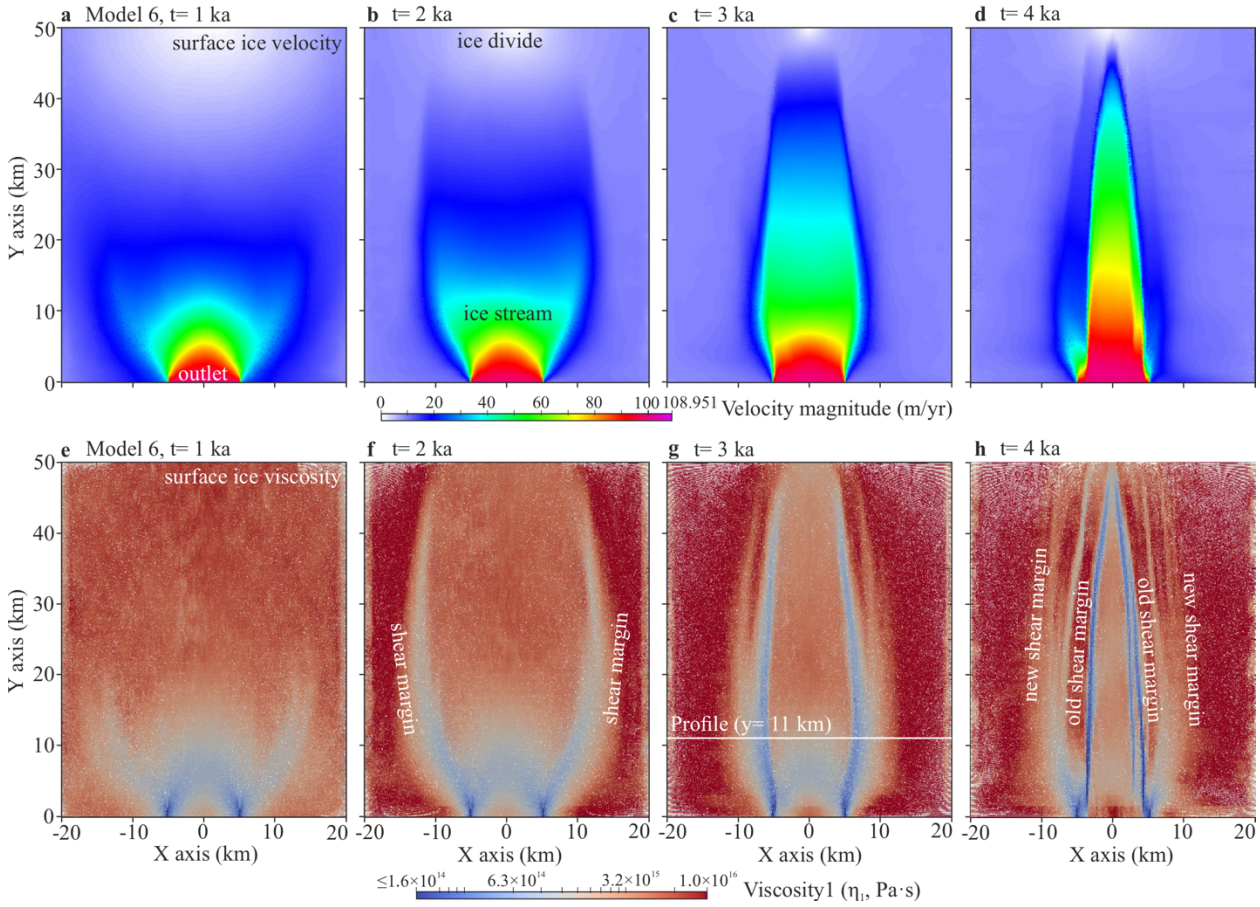

Fig. S20.

Evolution of surface ice velocities (**a–d**) and general viscosities η_1 (**e–h**) in Model 6 (free slip; symmetric inflow; anisotropy k = 100) from 1000 to 4000 years. The evolution process of the ice stream in Model 6 is faster than in Model 4 (k = 10; Fig. S18). The ice stream is well-developed in 2000 years with distinct shear margins close to the ice divide. At 3000 years, the ice stream is narrower and has a larger velocity difference with surrounding ice than in Model 4, separated by softer shear margins. From 2000 to 4000 years, shear margin migration can be observed as well.

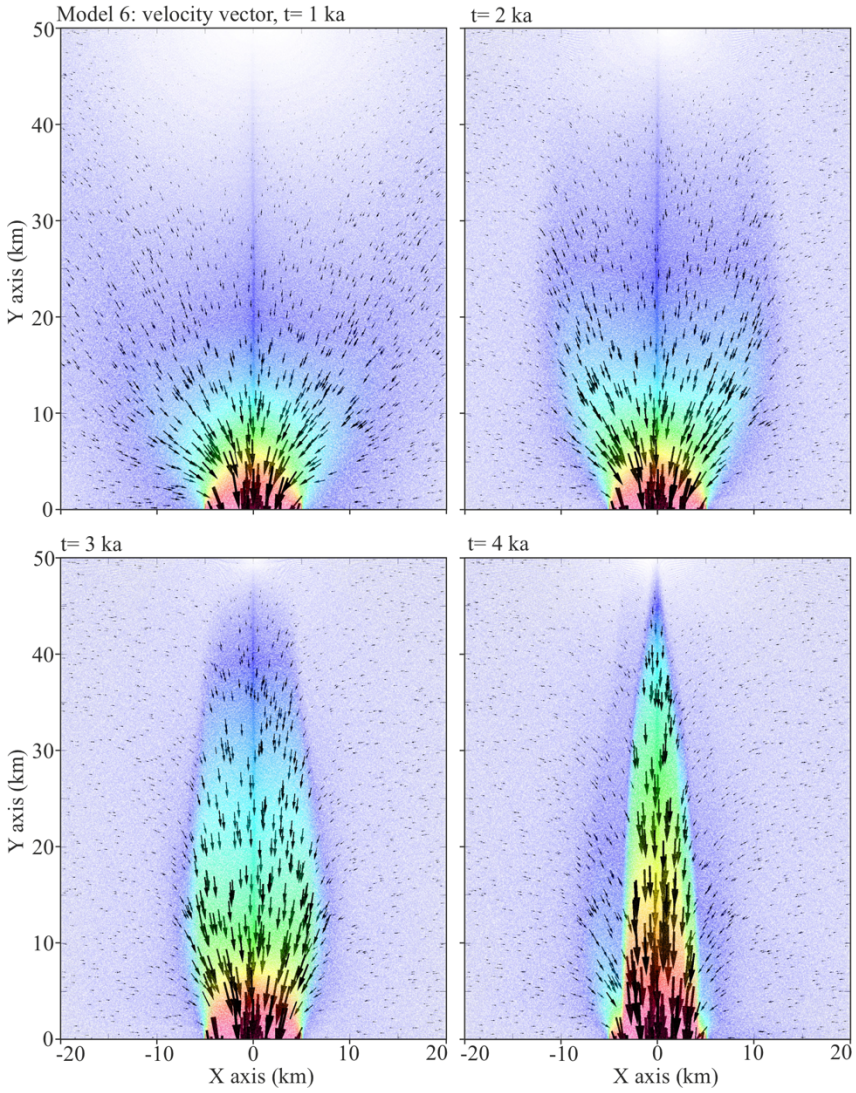

Fig. S21.

Top views of ice velocity vectors (arrows) in Model 6 from 1000 to 4000 years. Arrow orientations point to ice flow directions. The arrow size is scaled with ice flow speed. Ice stream position is shown with the translucent velocity magnitude map from Fig. S20. This model clearly shows the velocity vector field around a single ice stream changes through time.

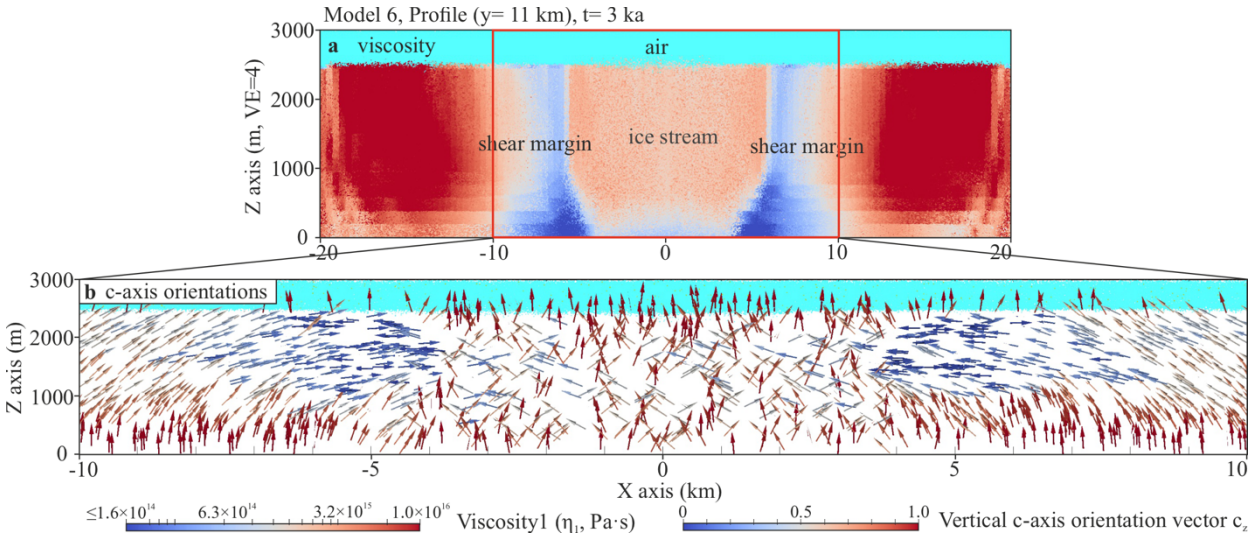

Fig. S22.

Profile snapshots of the single ice stream in Model 6 at 3000 years. Profile location is in Fig. S20. **a,** Ice general viscosities η_1 transverse the ice stream. Note the vertical exaggeration (4×) in the profiles. **b,** C-axis orientations (arrows) of ice particles around the ice stream marked in profile (**a**) with red frames. Arrow colours represent vertical vectors. This single ice-stream model has a larger distance between lateral model boundaries (*y*-walls) and its shear margins. With less boundary effect, the c-axis orientation patterns in and near both shear margins are more distinct. Except for the basal ice, c-axis orientations of ice particles inside and around shear margins are rotated towards the horizontal or small angles to the horizontal plane.

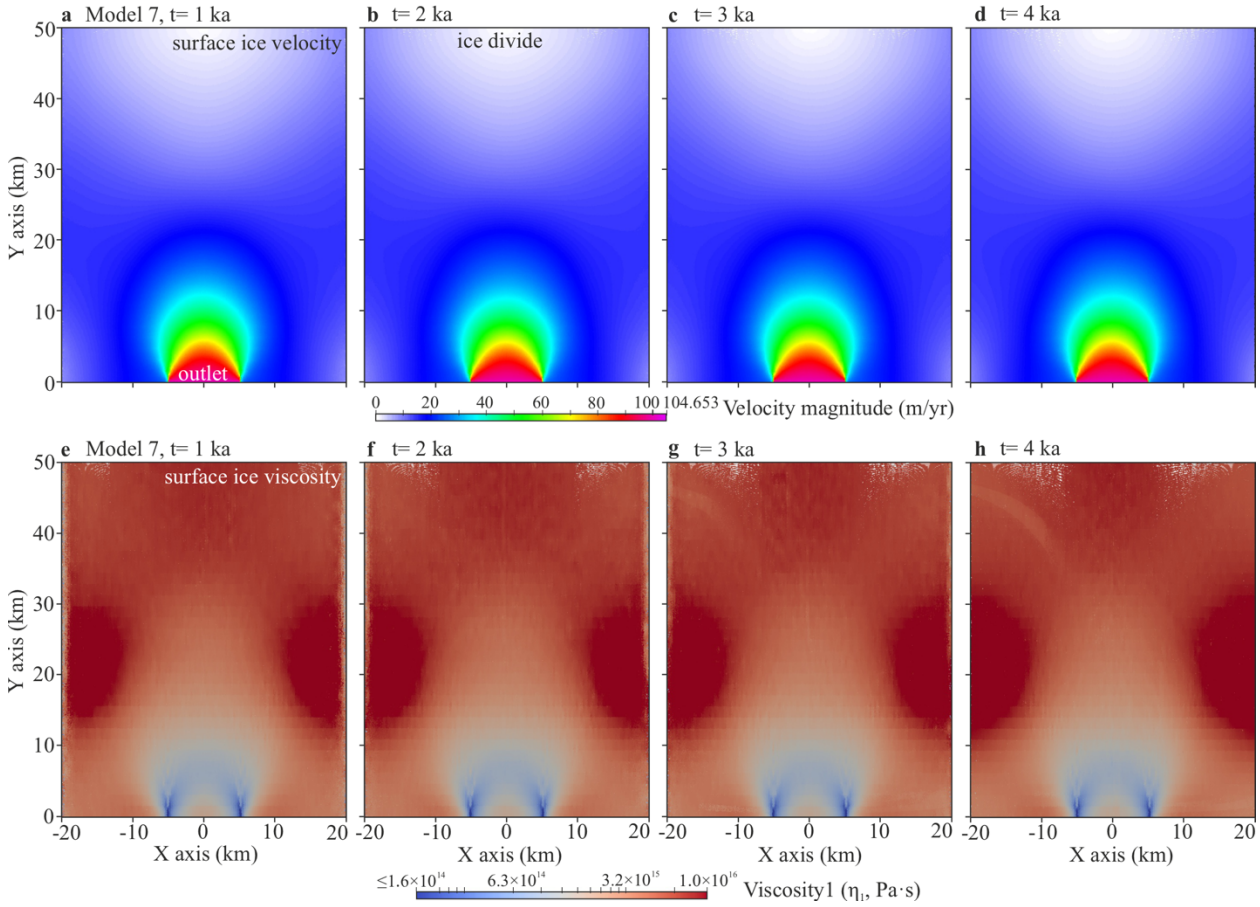

Fig. S23.

Evolution of surface ice velocities (**a–d**) and isotropic viscosities η_1 (**e–h**) in Model 7 (free slip; symmetric inflow; isotropy) from 1000 to 4000 years. However, shear margins cannot be established under our model conditions (even on a slippery bed), and no ice stream forms.

References

63. MacGregor, J. A. et al. A synthesis of the basal thermal state of the Greenland Ice Sheet. J. Geophys. Res. Earth Surf. 121, 1328–1350 (2016). doi:10.1002/2015JF003803
64. Hvidberg, C. S. et al. Surface velocity of the Northeast Greenland Ice Stream (NEGIS): assessment of interior velocities derived from satellite data by GPS. *Cryosphere* **14**, 3487–3502 (2020). doi:10.5194/tc-14-3487-2020
65. Holschuh, N., Lilien, D. A. & Christianson, K. Thermal weakening, convergent flow, and vertical heat transport in the Northeast Greenland Ice Stream shear margins. *Geophys. Res. Lett.* **46**, 8184–8193 (2019). doi:10.1029/2019GL083436
66. Hunter, P., Meyer, C., Minchew, B., Haseloff, M. & Rempel, A. Thermal controls on ice stream shear margins. *J. Glaciol.* **67**, 435–449 (2021). doi:10.1017/jog.2020.118
67. Perol, T., Rice, J. R., Platt, J. D. & Suckale, J. Subglacial hydrology and ice stream margin locations. *J. Geophys. Res. Earth Surf.* **120**, 1352–1368 (2015). doi:10.1002/2015JF003542
68. Keisling, B. A. et al. Basal conditions and ice dynamics inferred from radar-derived internal stratigraphy of the northeast Greenland ice stream. *Ann. Glaciol.* **55**, 127–137 (2014). doi:10.3189/2014AoG67A090
69. Fahnestock, M. A. et al. Ice-stream-related patterns of ice flow in the interior of northeast Greenland. *J. Geophys. Res. Atmos.* **106**, 34035–34045 (2001). doi:10.1029/2001JD900194
70. Raymond, C. F. Deformation in the vicinity of ice divides. *J. Glaciol.* **29**, 357–373 (1983). doi:10.3189/S0022143000030288
71. Alley, K. E., Scambos, T. A., Alley, R. B. & Holschuh, N. Troughs developed in ice-stream shear margins precondition ice shelves for ocean-driven breakup. *Sci. Adv.* **5**, eaax2215 (2019). doi:10.1126/sciadv.aax2215
72. Grinsted, A. et al. Accelerating ice flow at the onset of the Northeast Greenland Ice Stream. *Nat. Commun.* **13**, 5589 (2022). doi:10.1038/s41467-022-32999-2

Other Supplementary Materials

Video S1.

Tributary-type ice stream evolution in Model 1. This video shows the whole evolution process of surface ice velocities in Model 1 (no slip; symmetric inflow; anisotropy $k = 10$) from 0 to 5000 years (also see Fig. S3).

Video S2.

NEGIS-type ice stream evolution in Model 2. This video shows the whole evolution process of surface ice velocities in Model 2 (no slip; asymmetric inflow; anisotropy $k = 10$) from 0 to 5000 years (also see Fig. S7).

Video S3.

NEGIS-type ice stream evolution in Model 3. This video shows the whole evolution process of surface ice velocities in Model 3 (no slip; asymmetric inflow; anisotropy $k = 100$) from 0 to 4000 years (also see Fig. S13)..

Video S4.

Single ice stream evolution in Model 6. This video shows the whole evolution process of surface ice velocities in Model 6 (free slip; symmetric inflow; anisotropy $k = 100$) from 0 to 4000 years (also see Fig. S20).